Simulations of the Summer Circulation over the South American Region with an Eta Coordinate Model

SILVIO NILO FIGUEROA, PRAKKI SATYAMURTY, AND PEDRO LEITE DA SILVA DIAS*

Center for Weather Prediction and Climatic Studies, National Institute for Space Studies, São José dos Campos, São Paulo, Brazil

(Manuscript received 15 April 1994, in final form 9 September 1994)

ABSTRACT

A multilevel limited-area primitive equations model in eta coordinate is used to simulate the effects of the Amazonian latent heat source and the Andean topography on the summer (December, January, February) circulation over the South American region. The observed circulation features, such as the Bolivian high and the trough near the coast of Northeast Brazil in the upper troposphere, the elongated South Atlantic convergence zone (SACZ) oriented northwest to southeast from the southern Amazon region into the Atlantic Ocean, and the subtropical anticyclones in the South Pacific and South Atlantic Oceans in the lower levels are well simulated. Although heating alone produces the SACZ, the mountain and the basic flow put it in the observed position. It is found that regular daily pulses of heating are necessary for the maintenance of the SACZ. The position and intensity of the SACZ change rather substantially from the no-mountain case to the mountain case, thus showing the importance of the effect of the Andes on determining the convergence zone.

1. Introduction

The atmospheric circulation in summer over the region of South America presents some well-defined regional-scale circulation systems such as the large anticyclone centered over Bolivia, also known as the Bolivian high, and a trough near the coast of Northeast Brazil in the upper troposphere (Virji 1981; Kousky and Kagano 1981; Kousky and Gan 1981). On many occasions the circulation associated with this upper trough becomes a closed vortex with a cold core and exercises a great influence on the rainfall distribution over Northeast Brazil and the surrounding oceanic areas. In the lower troposphere the trade winds in the equatorial Atlantic penetrate into the Amazon region and then turn anticyclonic east of the Andes mountains to flow southward and southeastward to 15°S, where the flow then becomes cyclonic in the central parts of the continent to form a low near 20°S. Figure 1 shows these circulation features in the upper (a) and the lower (b) troposphere for February 1993. The low-level anticyclonic circulation around the subtropical highs in the South Atlantic and the South Pacific Oceans are also seen in this figure.

Another important feature of the summer circulation in the South American region is a wide and long zone of convergence oriented northwest to southeast in the subtropics near the coast of southeast Brazil, projecting into the adjoining South Atlantic Ocean, known as the South Atlantic convergence zone (SACZ) (Kodama 1992). The SACZ can be seen in the mean monthly cloudiness charts as a bright band or in the mean monthly outgoing longwave radiation (OLR) charts as a band of minimum energy (Fig. 2) during the summer months (December, January, February). It can also be observed in the daily or hourly infrared satellite imagery as a frontal cloud band situated over the states of Minas Gerais, Espirito Santo, Rio de Janeiro, and São Paulo and the adjoining South Atlantic for periods ranging from 3 to 10 days. This band of high convective activity is connected to the region of more intense convection over the Amazon Basin, as is, for example, shown in Fig. 3. A wide and bright band of convective clouds across the southeastern coast of Brazil persisted for many days in the months of January and February 1993. Figure 3 shows the situation during 9 and 10 February at 1200 UTC.

Most of tropical and subtropical South America receives more than 50% of the total annual precipitation in the austral summer season (Figueroa and Nobre 1990) in the form of convective rain with a strong diurnal variation (Silva Dias et al. 1987). In the southern Amazon the daily rainfall amounts are of the order of 10 mm day^{-1} on the average over vast regions, reaching more than 30 mm day^{-1} in heavy rain episodes. Thus, the release of latent heat is a large source of heating in the region, and it is likely to be responsible for the regional circulation characteristics in summer.

* Current affiliation: Department of Meteorology, Institute of Astronomy and Geophysics, University of São Paulo, São Paulo, Brazil.

Corresponding author address: Dr. Prakki Satyamurty, CPTEC/INPE, C.P. 515, São José dos Campos, SP. CEP 12.201, Brazil.

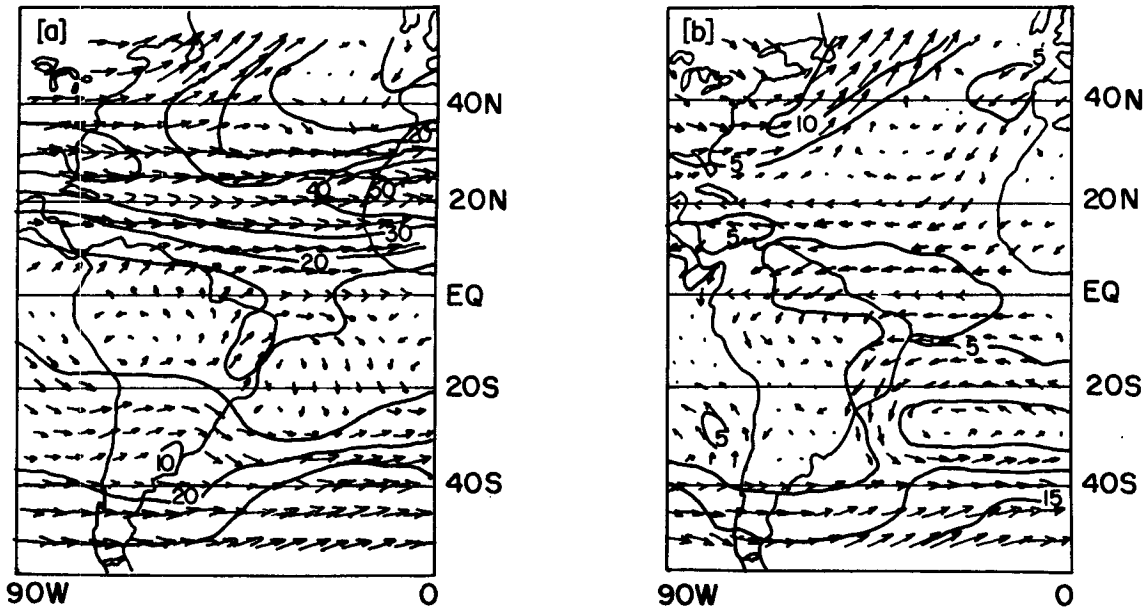

FIG. 1. Monthly mean vector winds and isotachs for February 1993 at 200 hPa (a) and 850 hPa (b) given by a National Meteorological Center analysis. Contour interval is 10 m s^{-1} [adapted from *Climate Diagnostics Bulletin* of the National Oceanic and Atmospheric Administration (NOAA) (Climate Analysis Center 1993)].

Previous model work has shown that the basic characteristics of the upper-tropospheric circulation can be reproduced by stationary and transient heat sources over the Amazon and central South America during the summer season (Silva Dias et al. 1983; DeMaria 1985; Paegle et al. 1987). The large tropical heat source has also been shown to have significant impact on the extratropical flow pattern (Kasahara and Silva Dias 1986; Paegle et al. 1987). Hoskins and Karoly (1981) and Simmons (1982) found the propagation of long waves from the tropical heat source toward polar regions to be an important mechanism of tropical–midlatitude interaction. Similar wave trains are also expected to emanate from South America during the summer season.

The regional low-level circulation over South America has not been adequately reproduced by the earlier numerical models. They have either ignored the topographical effect altogether (DeMaria 1985) or have included it in a simple fashion (Kleeman 1989). The interaction of the tropical heat source with topography may also be an important and interesting factor in determining the remote response of the heat source over tropical South America. However, the implementation of a numerical model for the South American region is rather complex because of the presence of the steep and narrow topography presented by the Andes.

Satyamurty et al. (1980) integrated a barotropic model with smooth topography and obtained a large stationary trough near southeastern Brazil in a meridionally varying midtropospheric zonal flow. Moderate to strong westerly winds in the subtropics forced to rise over the Andes, conserving potential vorticity, would produce a wave with a half-wavelength of about 3000 km east of the mountains. The effect of topography on the atmospheric circulation over South America was also studied by Kleeman (1989) from the point of view of Rossby and Kelvin wave scattering with an analyt-

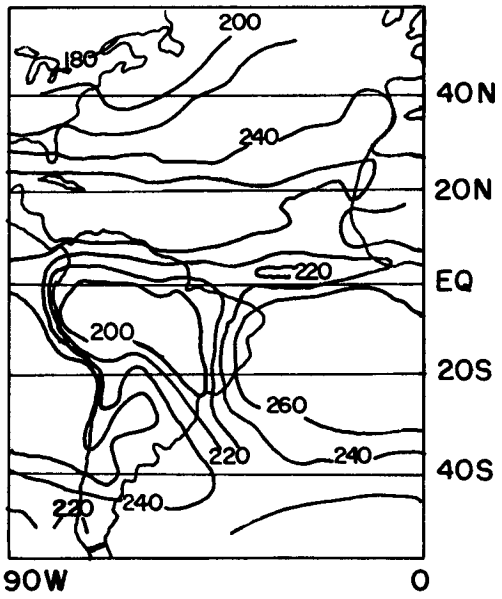

FIG. 2. Monthly mean outgoing longwave radiation for February 1993 obtained by *NOAA-11* Advanced Very High Resolution Radiometer (AVHRR) IR window (contour interval 20 W m^{-2}) (adapted from *Climate Diagnostics Bulletin* of NOAA).

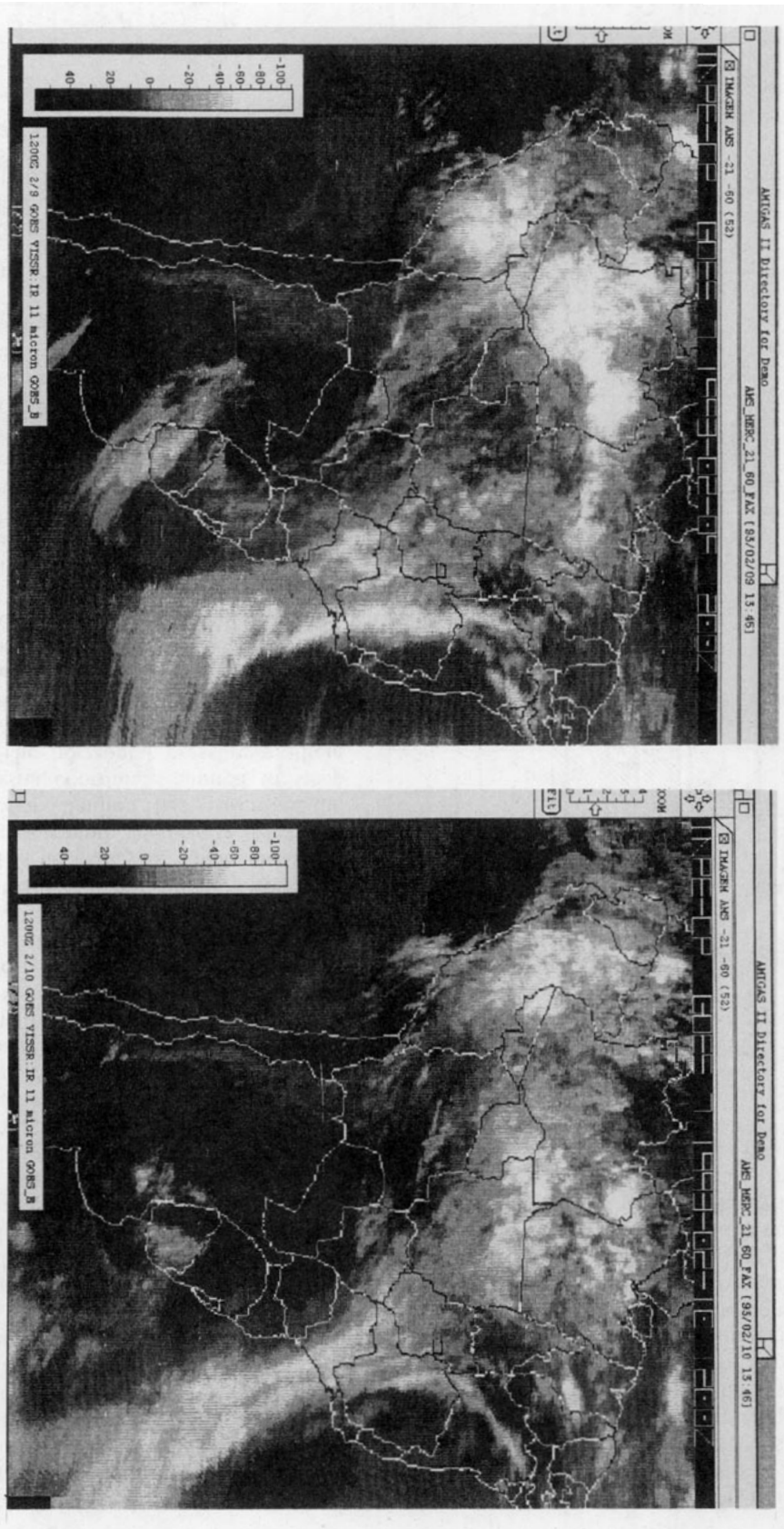

FIG. 3. *GOES-E* satellite IR (11 micron) imagery for the South American region at 1200 UTC for two consecutive days: (a) 9 February and (b) 10 February 1993. A wide and bright band of convective clouding, characterizing the South Atlantic convergence zone (SACZ), is seen to persist across the southeastern coast of Brazil.

ical model based on the long-wave approximation. Numerical solutions without the long-wave approximation were also considered by Kleeman with a simple two-level primitive equation model with the Andes represented by a knifelike barrier in the lower layer. Kleeman showed that the impact of topography remains confined to the lower troposphere in the timescale of a few days and that (a) internal Kelvin modes are reflected by the barrier, (b) incident internal Rossby modes are converted to external modes to the west of the Andes, and (c) low-level boundary jets are generated along the barrier as a result of back reflection of short Rossby waves. However, Kleeman expressed the necessity for generalizing the results to a full primitive equation model with many levels in which the height of the barrier is variable.

Gandu and Geisler (1992) experimented with a five-level sigma coordinate model including a prescribed diabatic heating function and produced some of the summer circulation features over the South American region, especially those in the upper troposphere. One feature that conspicuously escaped their attention was the SACZ.

In order to simulate the regional summer circulation more realistically, it is necessary to handle the steep topography of the region more adequately. Mesinger (1982) and Mesinger and Janjic (1985) discussed the problems of the sigma coordinate applied to steep mountain barriers. The horizontal pressure gradient force breaks into two large terms, which tend not to cancel each other to the degree they should, introducing errors that are generally larger for greater terrain slopes. Two different approaches to this problem have evolved: the envelope topography (Wallace et al. 1983) and the step-mountain topography (Mesinger 1984; Mesinger et al. 1988), of which the latter can easily be incorporated into the gridpoint models. Mesinger and Janjic (1985) developed an eta vertical coordinate, which eliminates the problems in the sigma coordinates near steep topography.

The present study proposes to make use of an eta coordinate model including the effect of the release of latent heat to simulate the observed regional-scale circulation features over South America, with special emphasis on the formation of SACZ.

2. Model description

The model uses the primitive equations with spherical horizontal coordinates and a vertical eta coordinate (Mesinger 1984) defined by

$$\eta = \frac{P - P_t}{P^*}, \tag{1}$$

where

$$P^* = \frac{P_s - P_t}{\eta_s}, \quad \eta_s = \frac{P_{rf}(z_s) - P_t}{P_{rf}(0) - P_t},$$

in which P is pressure; the subscripts s and t denote the values at the surface and at the top of the model atmosphere, respectively; z is height; z_s is the height of the top of mountain; and P_{rf} is a reference pressure at the top of mountain ($z = z_s$) or at the base of mountain ($z = 0$).

The governing equations of the model (Mesinger et al. 1988) are the u-momentum, the v-momentum, the thermodynamic energy, the mass continuity, the hydrostatic relation, and the surface pressure tendency equations, which form a closed set in the dependent variables u, v, T, P_s, ϕ, and $\dot{\eta}$, where the symbols have the usual meaning. The horizontal and vertical distributions of the variables in the presence of step mountains using grid C of Arakawa (Tokioka 1978) are shown in

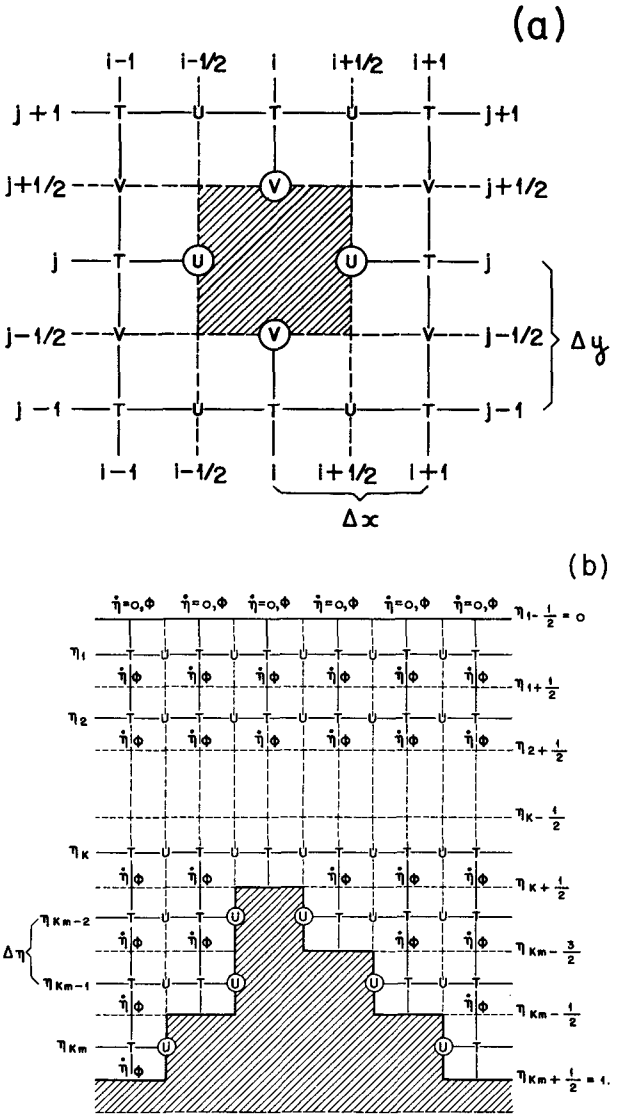

FIG. 4. Horizontal (grid C of Arakawa) (a) and vertical (b) grid sections. Hatched areas are mountain blocks.

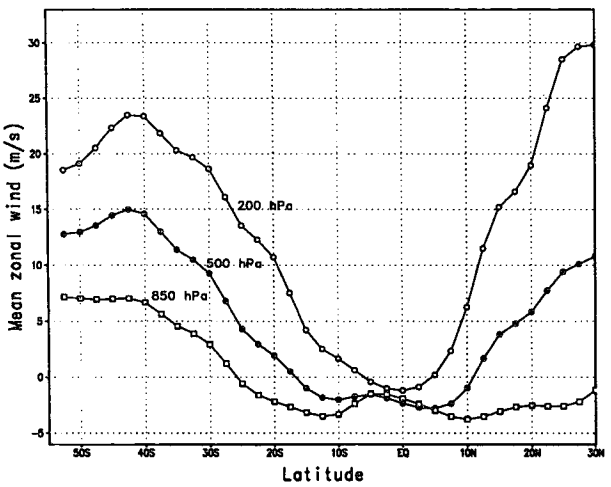

FIG. 5. Meridional profiles of zonally uniform basic-state wind at 850-, 500-, and 200-hPa levels.

Fig. 4, in which panel a is a horizontal section across a portion of the idealized mountain and panel b is a vertical section along a latitude circle over which the u component of the wind is defined. The variables u, v, and T are defined in levels η_k, which are referred to as principal levels; ϕ and $\dot{\eta}$ are defined in levels $\eta_{k+1/2}$, which are referred to as intermediate levels. The circle around the variables u and v indicates that the component perpendicular to the mountain is identically zero. The equations are discretized in the horizontal using the two-point differencing along with two-point averaging.

In limited-area models the horizontal boundary conditions pose problems, and therefore care has to be taken in their specifications to avoid false or spurious reflections of waves at the boundaries (Orlanski 1976). The open boundary condition proposed and tested by Orlanski is used at the east–west as well as north–south boundaries. The principal characteristic of this condition is to permit free passage of the waves generated in the interior of the domain and to block the entrance of the reflected waves into the domain. At the top and at the bottom of the model atmosphere (which is the same as the top of the mountain blocks), the vertical velocity $\dot{\eta}$ is specified to be zero.

The explicit leapfrog scheme is used for the integration in time for simplicity, and a five-point filter is applied with a weight 10 times less than the value needed for complete damping of the shortest waves. This damping is necessary in order to avoid noise caused by aliasing in view of the fact that no special effort is taken to conserve energy.

The domain of integration extends from 30°N to 55°S and from 150°W to 0°. The grid spacing in the horizontal is 2.5° latitude and longitude. In the vertical seven layers are used with the model top placed at the 20-hPa level. The time step for integration Δt is set equal to 300 s.

Two types of initial conditions are used: 1) atmosphere at rest and 2) zonally uniform flow obtained from the meridional and vertical profiles of temperature taken from Newell et al. (1972) and surface pressure taken from Godbole and Shukla (1981) for the South American region. Geostrophic balance is used to obtain the winds at all grid points except on the equator where the zonal wind is taken to be the mean of the two values to the north and south. The meridional profiles of the zonal-mean geostrophic winds at 850-, 500-, and 200-hPa levels are shown in Fig. 5.

3. Specification of the diabatic heating and the topography

In this study numerical experiments are conducted to obtain the response of the latent heat released in the region of intense convective activity over the central parts of the South American continent during summer. Examination of hourly satellite imagery indicates that this convection has a strong diurnal variation with limited activity in the morning, reaching explosive levels in the afternoon and early night hours (Silva Dias et al. 1987). The same is reflected in the seasonal-mean hourly rainfall distribution shown in Fig. 6. The heating is specified taking into account such a diurnal cycle.

Thus, the heating rate is specified to be

$$Q(x, y, z, t) = Q_{xy} Q_z Q_t, \qquad (2)$$

where $Q_{xy}(x, y)$, $Q_z(z)$ are nondimensional and give the form of the heating function in the horizontal and vertical domains, respectively. Here Q_{xy} is adapted from Silva Dias et al. (1983) and Q_z from DeMaria (1985) with a peak at 500 hPa. The horizontal distri-

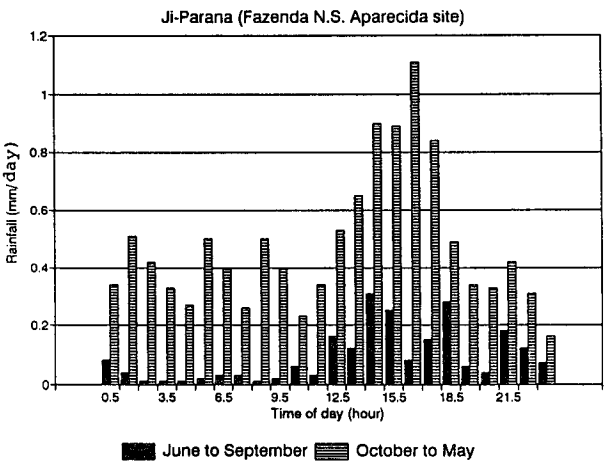

FIG. 6. Diurnal variation of seasonal mean precipitation rate at an Amazonian station, Ji-Parana (10° 47′S, 62° 22′W) obtained for 1991–93 during the Amazon Boundary Layer Experiment (courtesy of H. R. Rocha and his colleagues).

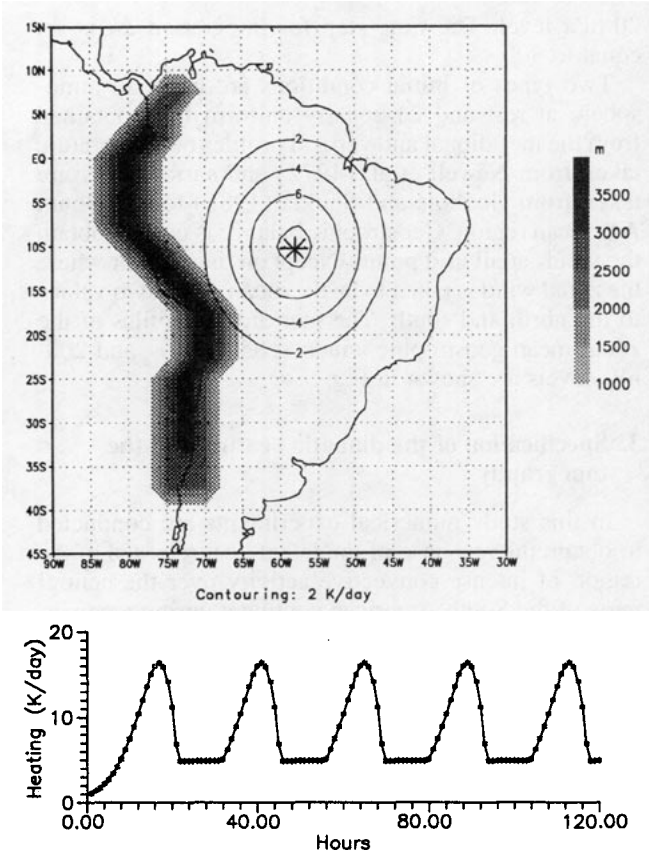

FIG. 7. Schematic representation of the horizontal (a) and temporal (b) distribution of diabatic heating. Step mountain topography is shown in (a).

bution of observed rainfall over the Amazon on a typical day has no well-defined shape but tapers off rapidly beyond the Amazon Basin and central Brazil. In this study Q_{xy} is given a circular shape with e-folding radius of 1000 km. The maximum heating rate is centered at 10°S, 58°W and 500 hPa, as is shown in Fig. 7a. The evolution of the heating, $Q_t(t)$, for five days is shown in Fig. 7b. The time referred to in this study is local time at the central point of the heating (i.e., 58°W) shown with a large asterisk in Fig. 7a. It can be seen that $Q_t(t)$ increases from 0800 local time (LT) to reach a peak of 17 K day^{-1} at 1700 LT and falls until 2100 LT to remain constant at 5 K day^{-1} until 0800 LT on the morning of the next day. However, in the beginning of the first day $Q_t(t)$ starts with a near-zero value to permit the model to adjust gradually to the heating. The heating rate values given in this graph correspond to an areal average over a 1000-km circle around the central point at the 500-hPa level. The function chosen is an approximation to the release of latent heat in the Amazon Basin corresponding to the rainfall distribution. The volume average value, over the portion of the atmosphere from surface to 10-km height within a radius of 1000 km from the central point (10°S, 58°W), of the specified heating function is approximately 8 K day^{-1}.

The model topography is shown in Fig. 7a. It consists of three mountain blocks with heights of 810, 2150, and 3950 m, corresponding to $\eta_{6+1/2}$, $\eta_{5+1/2}$, and $\eta_{4+1/2}$, respectively. The mountain is limited to 45°S in the south and 10°N in the north.

4. Simulations of the summer circulation over South America

Table 1 describes the characteristics of the experiments presented in the present study. Experiment 1 is used to evaluate the thermal circulation generated by heating alone. Experiment 2 is conducted to examine the interaction of the thermal circulation with topography. The interaction with the mean zonal flow of the resulting circulation is examined in experiments 3 and 4. Experiment 5 is conducted with a transient heat source in order to compare the performance of the present model with the results obtained by Kleeman (1989) and Gandu and Geisler (1992).

The evolutions of the model atmospheres in experiments 1, 2, 3, and 4 are presented through the wind and divergence fields at the 850-hPa (approximately $\eta = 0.846$) level and through the geopotential and wind fields at the 200-hPa (approximately $\eta = 0.183$) level, at noon on the fifth day of simulation—that is, 108 h after the start, for the area 45°S–15°N, 110°–10°W. The fields of the model atmosphere maintained the same basic characteristics after the first four days of simulation. The results are discussed in the subsections to follow.

a. Thermal circulation and its interaction with the Andes

The lower-tropospheric thermal circulation generated by the diabatic heating over the Amazon region and its modification by the Andean topography as seen by the present eta coordinate model are presented in Fig. 8. The diabatic heating has produced cyclonic cir-

TABLE 1. Characteristics of the experiments conducted.

Experiment	Characteristics
1	No mountain, rest initial state, heating as defined in Eq. (2).
2	Same as experiment 1 except for the inclusion of mountain.
3	Same as experiment 1 except for the inclusion of initial mean zonal flow.
4	Same as in experiment 2 except for the inclusion of initial mean zonal flow.
5	Same as in experiment 2 except for Q_t is specified as in Silva Dias et al. (1983) (single peak at 12 h).

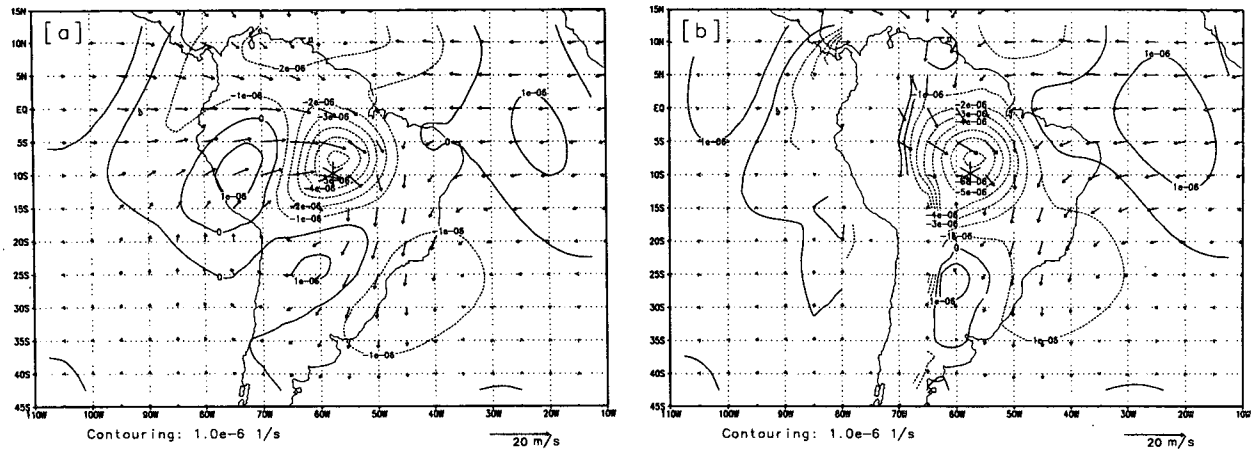

FIG. 8. Vector wind and divergence at 850 hPa: no-topography case (experiment 1) (a) and topography case (experiment 2) (b) at 1200 local time on day 5. Asterisk indicates the center of heat source.

culation centered at 17°S, 62°W with stronger winds on the northern and eastern sides and weaker winds on the southern and western sides (Fig. 8a). A region of strong convergence over the heat source in the Amazon and three regions of divergence, one to the west over Peru, one to the south over northern Argentina, and the other to the east in the tropical Atlantic, are produced. It is interesting to observe a rather weak but broad convergence region to the southeast of the source region near the southeastern coast of Brazil.

The changes resulting from the inclusion of topography (Fig. 8b) are as follows: (a) the winds in the equatorial belt east of the Andes changed direction to north-northwesterly; (b) the equatorial westerlies in the Pacific became very weak; (c) the convergence over the source region became more intense and it joined with the weak convergence region over the southeastern coast of Brazil; and (d) the divergence region over Peru almost disappeared.

The cyclonic circulation produced in the region of northern Argentina (Fig. 8b) corresponds to the "Chaco" low observed in summer (Schwertdfeger 1976). The broad region of low-level convergence oriented northwest to southeast emanating from the heat source region in Fig. 8b resembles the SACZ presented by Kodama (1992). It lies near the southwestern flank of the South Atlantic subtropical high and to the east of the Chaco low. It is interesting to note the agreement between the observed minimum OLR in Fig. 2 and the maximum low-level convergence in Fig. 8b with the mean position of SACZ given by Kodama (1993) in his Fig. 1.

The intensity of the low as seen from the cyclonic circulation in the region of northern Argentina in the

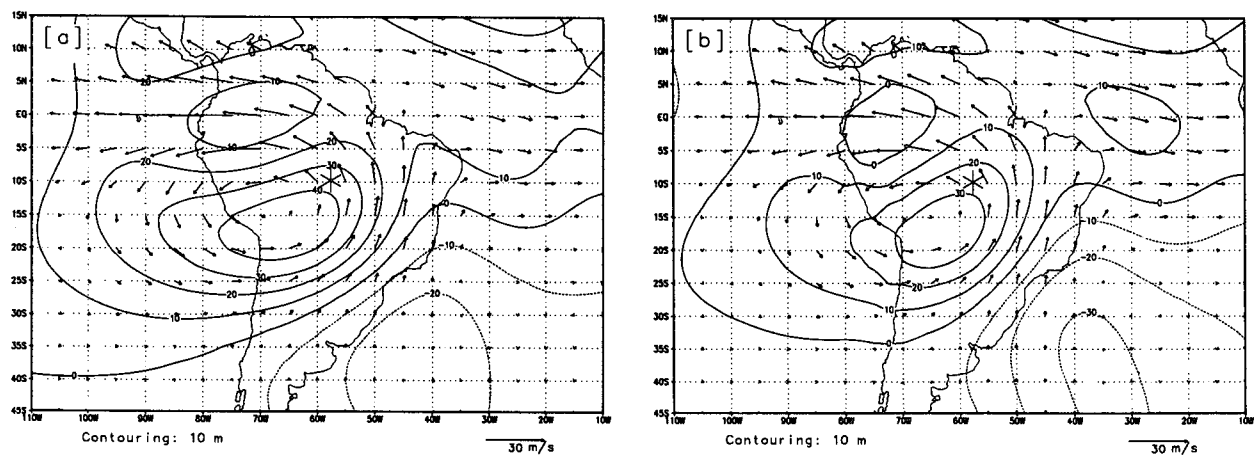

FIG. 9. Vector wind and deviation geopotential at 200 hPa: no-topography case (experiment 1) (a) and topography case (experiment 2) (b) at 1200 local time on day 5. Asterisk indicates the center of heat source.

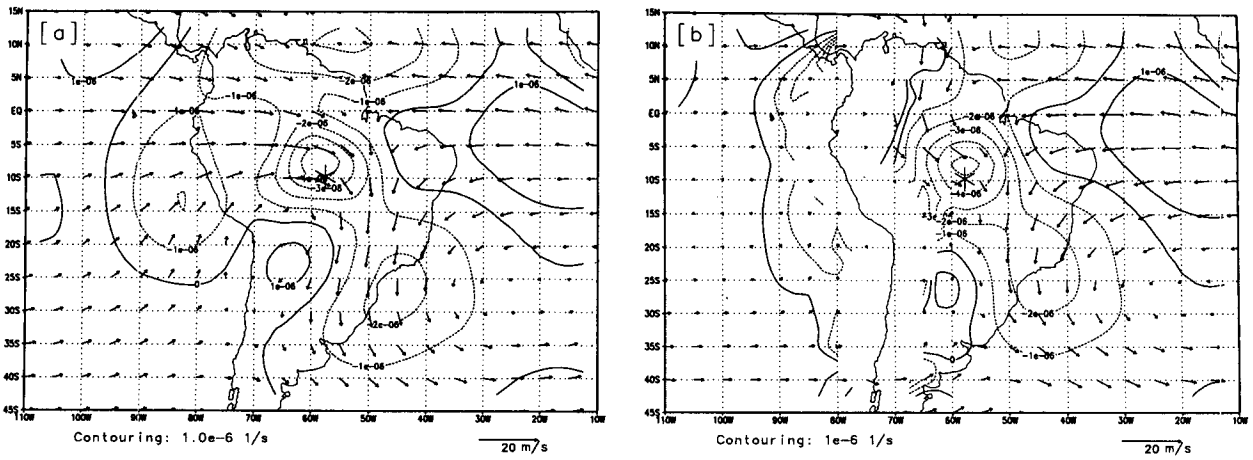

FIG. 10. Vector wind and divergence at 850 hPa in the cases with basic zonal flow: no-mountain case (experiment 3) (a) and mountain case (experiment 4) (b). Asterisk indicates the center of heat source.

present study (Fig. 8b) is somewhat less than the observed low (Fig. 1b), and its position is displaced a little to the north. Following the suggestion of Kleeman (1989) the center of the heat source is shifted to 12°S latitude in one experiment not presented here, but the result did not change significantly. It is expected that the diurnal radiational heating, which is not included in the model, is important for the formation of the Chaco low.

Figure 9 presents the characteristics of the model atmospheric flow in the upper troposphere. The heating produces a large anticyclone centered over Bolivia, approximately 10° south-southwest of the heat source, with stronger winds to the north, and a trough to the east over Northeast Brazil (Fig. 9a). Simulations made by many other authors (Silva Dias et al. 1983; DeMaria 1985; Gandu and Geisler 1992) with just one pulse of diabatic heating (denoted transient heat source) also produced similar major upper-tropospheric characteristics. The inclusion of topography decreased the intensity of the anticyclone (Fig. 9b), however, which maintained its position unaltered.

b. *Interaction of heat source with the mean zonal flow*

The interaction between the circulation generated by the Amazonian heat source and the basic zonal flow (experiment 3) and the modifications affected by the Andes mountains on the resulting circulation (experiment 4) are described in Figs. 10 and 11. Inclusion of a mean zonal basic flow without the effect of topography resulted in weaker 850-hPa convergence over the source region (Fig. 10a), but the convergence over southeastern Brazil intensified relative to the result shown in Fig. 8a. The low-level divergence west of the

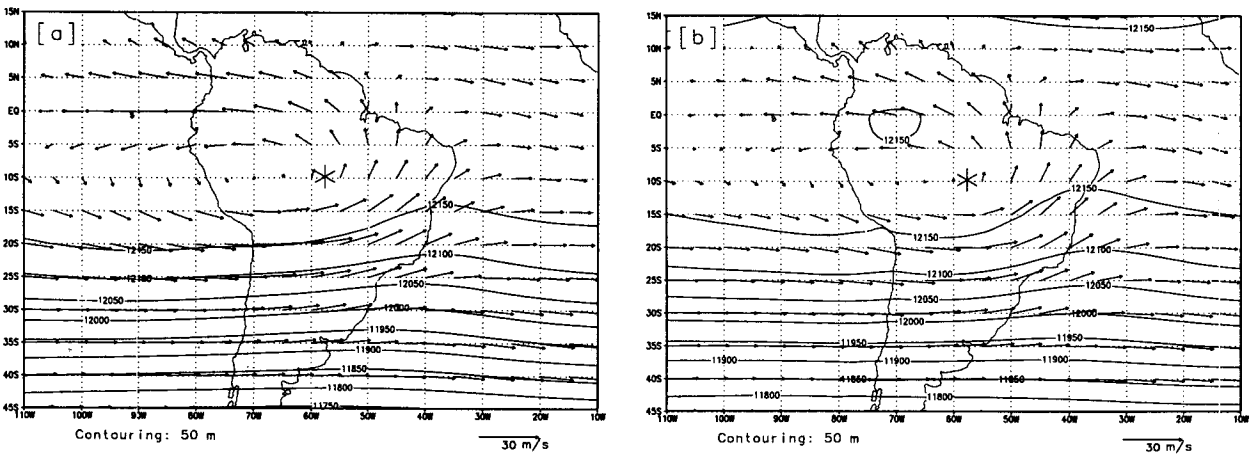

FIG. 11. Vector wind and deviation geopotential at 200 hPa in the cases with basic zonal flow: no-mountain case (experiment 3) (a) and mountain case (experiment 4) (b). Asterisk indicates the position of the center of heat source.

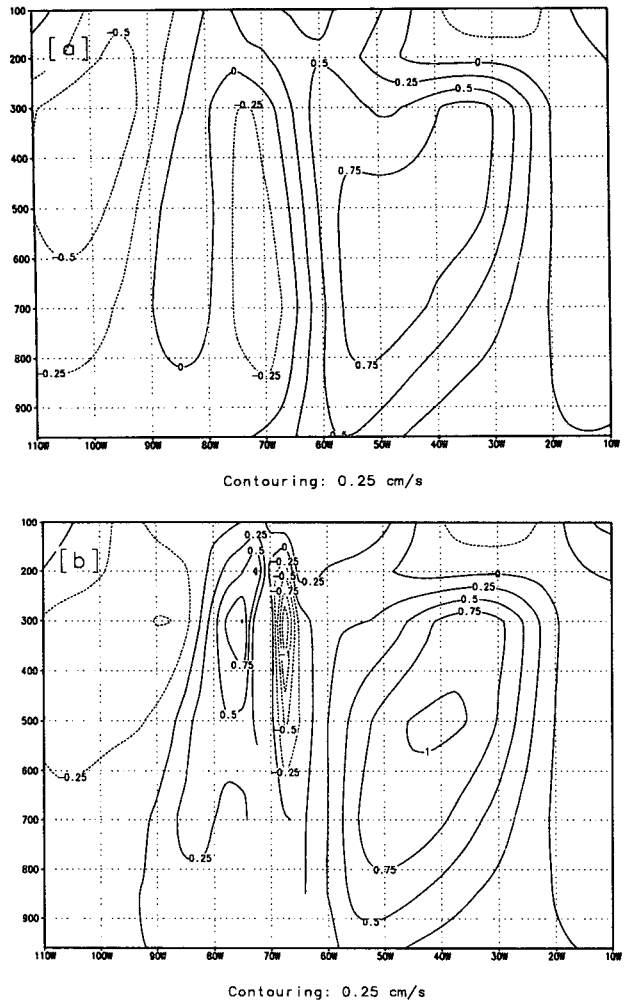

FIG 12. Vertical cross section of vertical velocity at 20°S in the case with mean zonal flow: no-mountain case (experiment 3) (a) and mountain case (experiment 4) (b). Units are in cm s^{-1}.

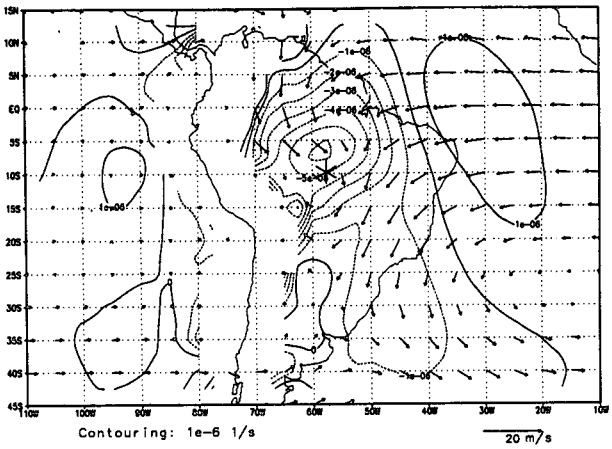

FIG. 13. Vector wind and divergence at 850 hPa in the case with mountain and mean zonal flow on day 5 at 0600 local time (experiment 4).

source region centered over Peru (Fig. 8a) is nonexistent in this experiment, and the divergence in the equatorial Atlantic has penetrated into Northeast Brazil. It is important to note that, when topography is included (Fig. 10b), the convergence area corresponding to the SACZ becomes well defined and located in its observed position (compare with Fig. 2). Interestingly, another somewhat weaker convergence zone is generated to the northeast of the source region, which corresponds to an observed feature in the satellite cloud imagery (see, e.g., Fig. 1 of Kodama 1993). It is gratifying to observe that the lower-tropospheric flow features in Figs. 10b and 1b compare very well. The results presented in this case show effectively that the model is capable of producing the observed features in summer quite faithfully.

The upper-tropospheric flow characteristics in the case of heat source interaction with the mean zonal flow with and without topography are shown in Figs. 11a and 11b, respectively. The anticyclonic circulation corresponding to the Bolivian high is zonally elongated into the tropical Pacific, especially in the case of no topography. Comparing Figs. 11b and 9b it can be observed that the winds south of 15°S become stronger and more realistic. The geopotential lines become open to be consistent with the wind field. The trough to the northeast of the source region has slightly intensified when topography is included, as can be seen more clearly in the geopotential field. Comparing the flow field in Figs. 11b and 1a reveals that the often observed closed vortex off the northeastern coast of Brazil is not adequately reproduced by the model. It seems that the formation of the vortex depends on factors other than those considered in the model, such as Northern Hemispheric large-scale circulation features and other heat sources and sinks.

Figure 12 shows the vertical velocity field in a vertical section across 20°S obtained in experiments 3 and 4. It is necessary to remember that the mountain is situated approximately centered at 70°W at this latitude. The model produces ascending motion over a wide area from 60° to 20°W corresponding to the SACZ. It is interesting to note that the inclusion of topography intensifies the ascending motion, its maximum occurring at 40°W and 500-hPa level over the SACZ region. It can also be seen that the flow is ascending west of the mountain and descending immediately to the east.

In order to examine the structure of the convergence zone at a different hour of the day, the 850-hPa fields in experiment 4 at 0600 LT on the fifth day are presented in Fig. 13. One can see that the convergence is weaker in the region of SACZ and stronger in the source region compared to the 1200 LT field shown in Fig. 10b. This suggests that the intensity of SACZ pre-

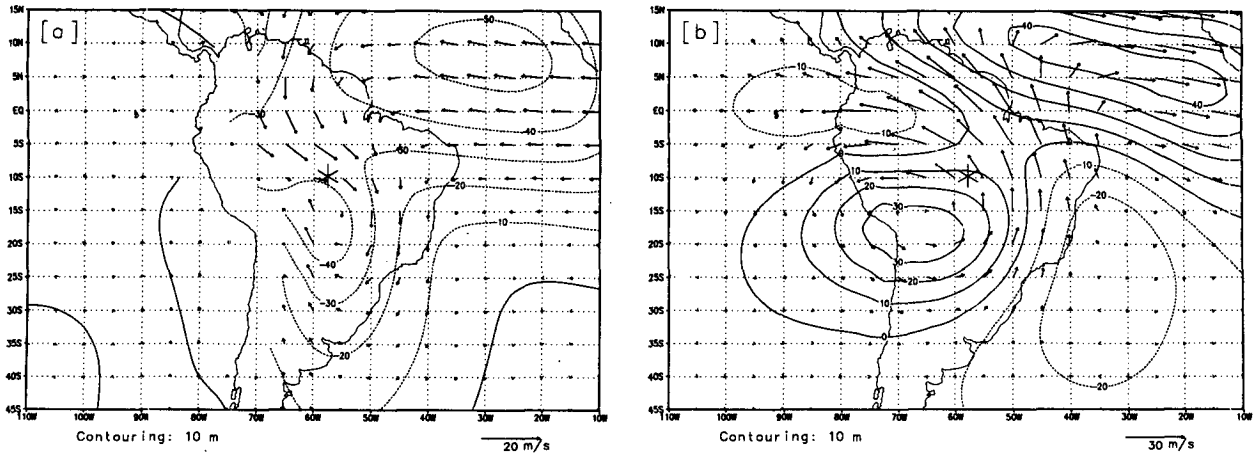

FIG 14. Vector wind and deviation geopotential in the case with mountain, initial rest state, and transient heating function (one pulse only) (experiment 5) at 42 h after the start of integration, corresponding to 30 h after the peak diabatic heating: 850-hPa level (a) and 200-hPa level (b).

sents a diurnal cycle similar to but perhaps not simultaneous with the convection over the Amazon region.

Experiments 3 and 4 are repeated using a slightly different initial flow field in which the zonal-mean geostrophic winds are substituted by the observed values in the equatorial region between 10°N and 10°S, and the results are almost identical to those shown previously.

From all the results presented above one can see that a convergence region is formed in the Atlantic near the southeastern coast of Brazil in the absence of the Andes, but the inclusion of the effect of topography makes it more realistic in its position, orientation, and intensity (Figs. 10a,b), thus representing the SACZ. The absence of the SACZ in the results of many earlier numerical simulations is perhaps due to the inadequate heating function and the absence of steep mountains.

c. *Experiments with single-impulse heating function*

Many authors (Silva Dias et al. 1983; DeMaria 1985; Kleeman 1989; Gandu and Geisler 1992) in the last 10 years have conducted experiments with a heating function containing just one peak. To compare the performance of the present model with their results, one run (experiment 5) is made with just one peak for the heating rate in which $Q_1(t)$ reaches a maximum 12 h after start and decays asymptotically to reach zero. Figures 14a and 14b show the wind and geopotential fields obtained in experiment 5 at 850 hPa and 200 hPa, respectively, at 42 h. The 850-hPa fields agree in many respects with the low-level fields presented in Figs. 8 and 9 of Kleeman. However, the winds in the region between the equator and 10°S and between 70° and 50°W produced in the lower levels by Kleeman (1989) are almost westerly, whereas they are northwesterly in the present experiment, which agrees more faithfully with the observed winds shown in Fig. 1b here and Fig. 1d of Kleeman (1989).

The formation of the SACZ occurs with this type of heating between 24 and 36 h, that is, 12 to 18 h after the peak heating, with a maximum at 30 h. Figure 15 shows the low-level divergence field in experiment 5 at 30 h. The convergence in this case is stronger than in Fig. 8b because the volume average heating rate in the first 30 h of integration is higher (about 15 K day^{-1}). Actually, the mean volume average heating rate over a period of 3 days is taken to be 8 K day^{-1}. After 36 h SACZ gets weakened and disorganized, which shows that it is important to have regular pulses of heating to maintain the SACZ in its intensity and position. This justifies our choice of heating function, shown in Fig. 7b, considered in experiments

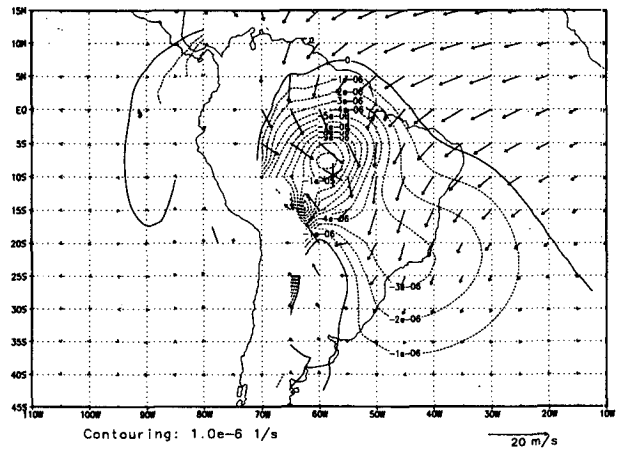

FIG. 15. Same as in Fig. 8a except at 32 h after the start of integration in experiment 5, corresponding to 20 h after the peak diabatic heating.

1 through 4. Experiments conducted with a constant heating rate (not shown here) produce a very weak SACZ or no SACZ.

The upper-level flow characteristics at 42 h (Fig. 14b) are very well defined and agree fairly well with the observed fields. There are differences between the present results and those obtained by Gandu and Geisler (1992) mainly because they have considered a latitudinally uniform basic-state flow. Comparing Figs. 14b and 9b reveals that a strong single-impulse (or transient) heating produces stronger westerlies over the equatorial Atlantic and that the Northeast Brazilian trough penetrates deeper into the continent.

5. Summary and conclusions

A primitive equation eta coordinate regional model is developed to study the effects of Amazonian diurnal convective activity on the summer circulation over the South American Tropics and subtropics. The specified heating rate has a half-sine function profile in the vertical, reaching a maximum at 500 hPa, and a circular shape in the horizontal, with an *e*-folding radius of 1000 km. In the time domain, the diabatic heating attains a maximum of 18 K day^{-1} at 1700 LT and falls off slowly thereafter until 2100 LT to remain constant at 5 K day^{-1} until 0800 LT, thus representing the diurnal cycle of the convective activity in summer over the southern Amazon region and central Brazil. Simulations with and without the steep mountain barrier and with and without the basic mean flow present substantial differences in the circulation features, especially in the lower troposphere, thus revealing the important role played by the Andes in modulating the regional atmospheric conditions.

The experiment with initial rest state has simulated well the regional summer circulation characteristics such as the upper-tropospheric Bolivian anticyclone, a low pressure center in the lower levels southwest of the heat source, a trough to the northeast of the Bolivian high, easterlies in the lower levels, and strong westerlies in the higher levels in the equatorial Atlantic.

An important feature of the simulated lower-tropospheric flow is the development of a long and fairly wide region of convergence, aligned northwest to southeast, from southeastern Amazonia into the South Atlantic (Fig. 10b), thus simulating the South Atlantic convergence zone (SACZ) studied by Kodama (1993).

The SACZ is frequently observed during summer and occasionally persists for up to 10 days (Satyamurty and Rao 1988); it can be seen in the monthly or seasonal outgoing longwave radiation (OLR) charts as a band of maximum convective activity or minimum energy, as, for example, in Fig. 2. The model reproduces a similar feature, in approximately the right place, by the combined effect of the diabatic heating over the Amazon/central Brazil and the steep Andean topography. The inclusion of the climatological basic flow introduces some minor but significant modifications on the location of the lower-tropospheric convergence zone. The agreement between the low-level convergence in Fig. 10b and the observed location of SACZ (Fig. 1 of Kodama 1993) clearly shows that the mechanism for the generation of the SACZ is indeed the combined action of Amazonian latent heat source and the steep Andean topography on the regional basic flow. The magnitude of the 850-hPa convergence in the model SACZ is slightly more than 2×10^{-6} s^{-1}, which compares well with the approximate observed value of 3×10^{-6} s^{-1} for the pentad 15–19 February 1988 obtained from the European Centre for Medium-Range Weather Forecasts (ECMWF) 1200 UTC analyses.

A very prominent convergence zone similar to SACZ in the Pacific is known as the South Pacific convergence zone (SPCZ), which is studied by Kiladis et al. (1989). They suggested the warmer sea surface temperatures (SST) as one of the possible mechanisms for the origin of SPCZ. In the case of SACZ this does not seem to be the case, because the position of the band of maximum convection as seen in Fig. 2 is different from the position of the warm water tongue in the Atlantic as shown in Fig. 16. Therefore, it appears that for the generation of the SACZ the SST is not very important. Another mechanism for the SACZ could be the remote excitation by the upstream SPCZ as is suggested by Kalnay et al. (1986). The regional model used in the present study has limited horizontal extention and cannot take this effect into account.

The position and intensity of the model SACZ depends on whether the growth of diurnal convection is

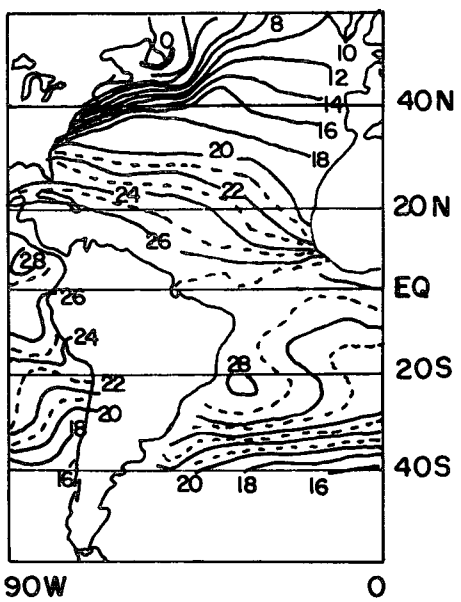

FIG. 16. Sea surface temperature in the South Atlantic Ocean region adjoining South America for February 1993. Contour interval is 2°C.

transient or persistent. Thus, the experiments suggest that monitoring of the convection characteristics over the Amazon is useful in forecasting subsequent convective activity in central-western and southeastern Brazil and adjoining regions.

This study has a few limitations: dry model, limited area, absence of diurnal radiational heating and air–sea interactions, and no upward cumulus momentum transport. In spite of the limitations, the forced dynamics alone was able to produce many features of the regional circulation over South America and show the importance of the interaction between the effects of Amazonian diabatic heating and steep Andes mountains on the atmospheric flow.

Acknowledgments. The authors wish to thank Drs. V. Innocentini, V. E. Kousky, and A. D. Moura for critically going through the manuscript.

REFERENCES

Climate Analysis Center, 1993: *Climate Diagnostics Bulletin.* National Meteorological Center, National Oceanic and Atmospheric Administration, U. S. Department of Commerce, 72 pp.

DeMaria, M., 1985: Linear response of a tropical atmosphere to convective forcing. *J. Atmos. Sci.,* **42,** 1944–1959.

Figueroa, S. N., and C. A. Nobre, 1990: Precipitation distribution over central and western tropical South America. *Climanálise,* **5,** 36–45.

Gandu, A. W., and J. E. Geisler, 1992: A primitive equations model study of the effect of topography on the summer circulation over tropical South America. *J. Atmos. Sci.,* **48,** 1822–1836.

Godbole, R. V., and J. Shukla, 1981: Global analysis of January and July sea level pressure. NASA-TM-82097, National Academy of Sciences, Washington, DC, 53 pp.

Hoskins, B. J., and D. J. Karoly, 1981: The steady linear response of a spherical atmosphere to thermal and orographic forcing. *J. Atmos. Sci.,* **45,** 585–604.

Kalnay, E., K. C. Mo, and J. Peagle, 1986: Large-amplitude, short-scale stationary Rossby waves in the Southern Hemisphere: Observations and mechanistic experiments to determine their origin. *J. Atmos. Sci.,* **43,** 252–275.

Kasahara, A., and P. L. Silva Dias, 1986: Response of planetary waves to stationary tropical heating in a global atmosphere with meridional and vertical shear. *J. Atmos. Sci.,* **43,** 1893–1911.

Kiladis, G. N., H. von Storch, and H. van Loon, 1989: Origin of the South Pacific convergence zone. *J. Climate,* **2,** 1185–1195.

Kleeman, R., 1989: A modeling study of the effect of the Andes on the summertime circulation of tropical South America. *J. Atmos. Sci.,* **46,** 3344–3362.

Kodama, Y.-M., 1992: Large-scale common features of subtropical precipitation zones (the Baiu frontal zone, the SPCZ, and the SACZ). Part I: Characteristics of subtropical frontal zones. *J. Meteor. Soc. Japan,* **70,** 813–836.

——, 1993: Large-scale common features of subtropical precipitation zones (the Baiu frontal zone, the SPCZ, and the SACZ). Part II: Conditions of the circulations for generating the STCZs. *J. Meteor. Soc. Japan,* **71,** 581–610.

Kousky, V. E., and M. A. Gan, 1981: Upper tropospheric cyclonic vortices in the tropical South Atlantic. *Tellus,* **33,** 538–550.

——, and M. T. Kagano, 1981: A climatological study of the tropospheric circulation over the Amazon region. *Acta Amazonica,* **11,** 743–758.

Mesinger, F., 1982: On the convergence and error problems of the calculation of the pressure gradient force in sigma coordinate models. *Geophys. Astrophys. Fluid Dyn.,* **19,** 105–107.

——, 1984: A blocking technique for representation of mountains in atmospheric models. *Revista di Meteorologica Aeronautica,* **XLII,** 196–202.

——, and Z. I. Janjic, 1985: Problems and numerical methods of the incorporation of mountains in atmospheric models. *Lect. Appl. Math.,* **22,** 81–120.

——, ——, S. Nickovic, D. Gavrilov, and D. Deaven, 1988: The step-mountain coordinate: Model description and performance for cases of Alpine lee cyclogenesis and for a case of an Appalachian redevelopment. *Mon. Wea. Rev.,* **116,** 1493–1518.

Newell, R. E., J. W. Kidson, D. G. Vincent, and G. J. Boer, 1972: *The General Circulation of the Tropical Atmosphere and Interactions with Extratropical Latitudes.* Vol. 1. MIT Press, 258 pp.

Orlanski, I., 1976: A simple boundary condition for unbounded hyperbolic flows. *J. Comput. Phys.,* **21,** 251–256.

Paegle, J., C. D. Zhang, and D. P. Baumhefner, 1987: Atmospheric response to tropical thermal forcing in real data integrations. *Mon. Wea. Rev.,* **115,** 2975–2995.

Satyamurty, P., and V. B. Rao, 1988: Zona de convergencia do Atlantico Sul (South Atlantic convergence zone). *Climanálise,* **3,** 31–35.

——, R. P. Santos, and M. A. M. Lemes, 1980: On the stationary trough generated by the Andes. *Mon. Wea. Rev.,* **108,** 510–519.

Schwertdfeger, W., 1976: The atmospheric circulation over Central and South America. *World Survey of Climatology,* Vol. 12. W. Schwertdfeger and H. E. Landsberg, Eds., Elsevier, 1–12.

Silva Dias, P. L., W. H. Schubert, and M. DeMaria, 1983: Large-scale response of the tropical atmosphere to transient convection. *J. Atmos. Sci.,* **40,** 2689–2707.

——, J. P. Bonatti, and V. E. Kousky, 1987: Diurnally forced tropical tropospheric circulation over South America. *Mon. Wea. Rev.,* **115,** 1465–1478.

Simmons, A. J., 1982: The forcing of stationary wave motion by tropical diabatic heating. *Quart. J. Roy. Meteor. Soc.,* **108,** 503–534.

Tokioka, T., 1978: Some considerations on vertical differencing. *J. Meteor. Soc. Japan,* **56,** 98–111.

Virji, H., 1981: A preliminary study of summertime tropospheric circulation patterns over South America estimated from cloud winds. *Mon. Wea. Rev.,* **109,** 599–610.

Wallace, J. M., S. Tibaldi, and A. J. Simmons, 1983: Reduction of systematic forecast errors in the ECMWF model through the introduction of an envelope orography. *Quart. J. Roy. Meteor. Soc.,* **109,** 683–717.